FISSION FOIL MEASUREMENTS OF NEUTRON AND PROTON FLUENCES IN THE A0015 EXPERIMENT*

A.L. Frank and E.V. Benton
Eril Research, Inc.
P. O. Box 150788
San Rafael, CA   94915-0788, U.S.A.

T. W. Armstrong and B.L. Colborn
Science Applications International Corporation
Route 2, Prospect, TN   38477, U.S.A.

SUMMARY

Results are given from sets of fission foil detectors (FFDs) (^{181}Ta, ^{209}Bi, ^{232}Th, ^{238}U) which were included in the A0015 experiment to measure combined proton/neutron fluences. Use has been made of recent FFD high energy proton calibrations for improved accuracy of response. Comparisons of track density measurements have been made with the predictions of environmental modeling based on simple 1-D (slab) geometry. At 1 g/cm^2 (trailing edge) the calculations were $\sim$25% lower than measurements; at 13 g/cm^2 (Earthside) calculations were more than a factor of 2 lower. A future 3-D modeling of the experiment is needed for a more meaningful comparison. Approximate mission proton doses and neutron dose equivalents were found. At Earthside (13 g/cm^2) the dose was 171 rad and dose equivalent was 82 rem. At the trailing edge (1 g/cm^2) dose was 315 rad and dose equivalent was 33 rem. The proton doses are less than expected from TLD doses by 16% and 37%, respectively. These differences can be explained by uncertainties in the proton and neutron spectra and in the method used to separate proton and neutron contributions to the measurements.

INTRODUCTION

The A0015 radiation experiment consisted of sets of passive integrating detectors which were contained in three different sealed canisters on the LDEF satellite. Canisters #1 and #2 (at the Earth end and near the trailing edge of LDEF, respectively) were filled with the detectors while Canister #3 (near the trailing edge) was only partially filled. Both #1 and #2 carried a selection of FFDs. The FFDs consist of heavy metal foils in contact with muscovite mica films. The foil types included ^{181}Ta, ^{209}Bi, ^{232}Th and ^{238}U.
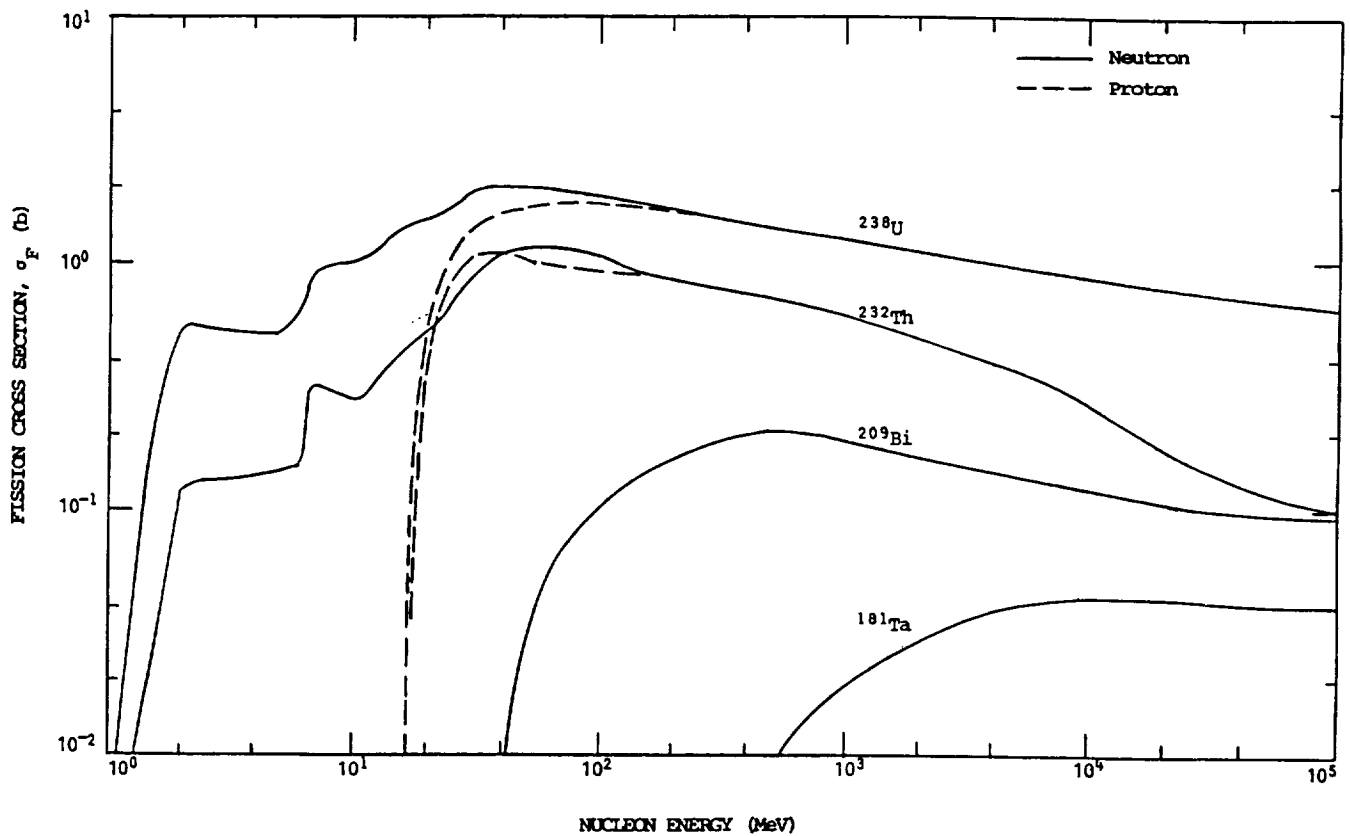

Figure 1: Fission cross sections for neutrons and protons incident on heavy metal foils.

Heavy metal nuclei have significant cross sections for fission when irradiated with neutrons and protons. Each isotope is characterized by threshold energies for the fission reactions and particular energy-dependent cross sections. In the FFDs, fission fragments produced by the reactions are emitted from the foils and create latent particle tracks in the adjacent mica films. When the films are processed, surface tracks are formed which can be optically counted. The track densities are indications of the fluences and spectra of neutrons and/or protons.

FFDs have previously been used for spaceflight measurements[4, 2, 3, 6, 5]. In cases where the proton contribution to track densities can be subtracted out, the FFDs can be used as high energy (>1 MeV) neutron dosimeters. These detectors have been calibrated with neutrons of energies up to ~15 MeV and found to have efficiencies ϵ = 1.16 × 10^{-5} tracks/neutron barn[8]. More recently, calibrations have been performed with high energy protons. At high energies, either proton or neutron calibrations are sufficient since the cross section data, plotted in Figure 1[7, 10, 9], show that the proton and neutron fission cross sections are approximately equal.

Detector efficiencies, plotted in Figure 2, have been found for the four FFD types by combining low
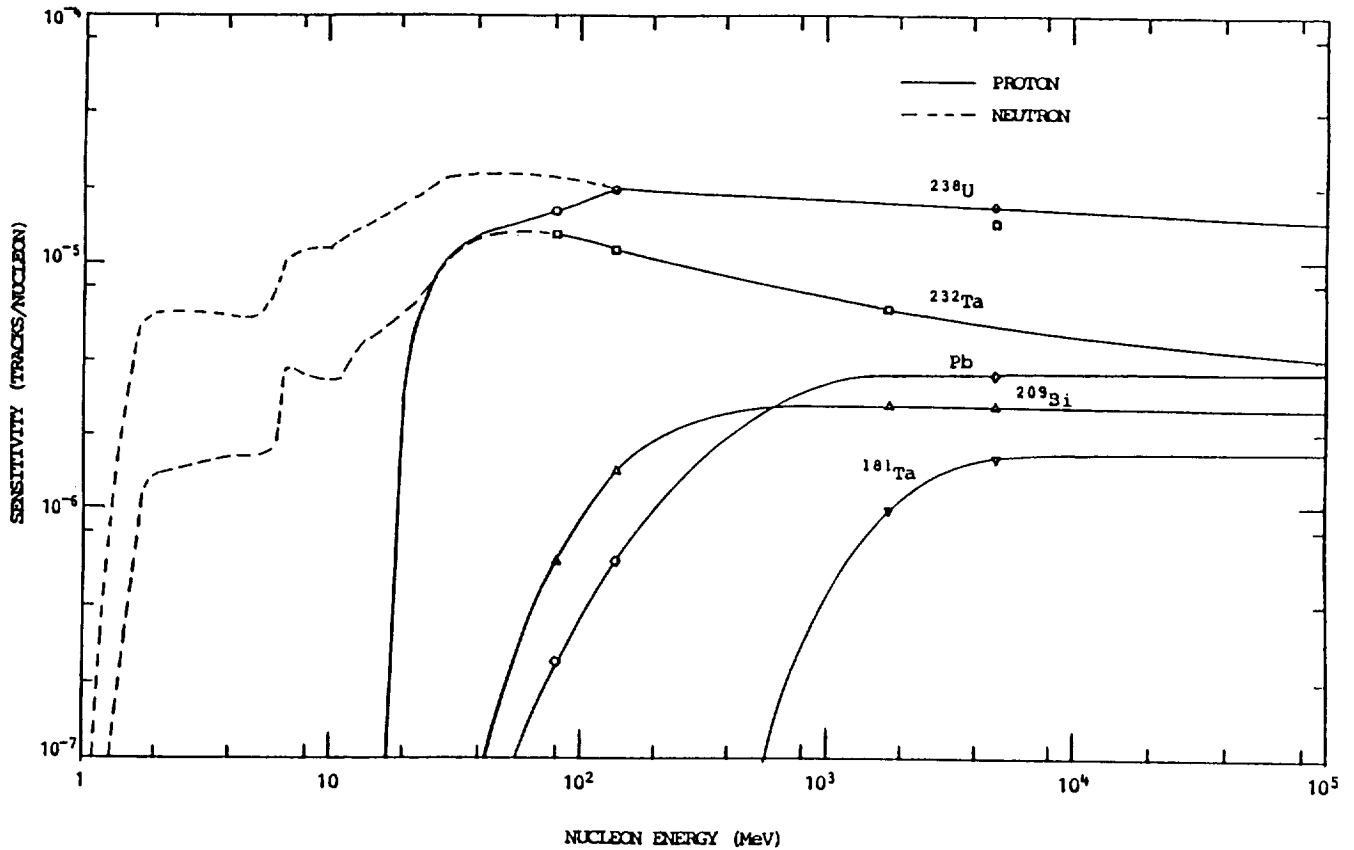
Figure 2: Sensitivities of fission foil detectors to neutrons and protons.

energy neutron and high energy proton calibrations with the published fission cross sections to cover the energy region from 1 MeV to 100 GeV. Armstrong and Colborn[1] have shown that the energy range of interest in space applications extends to 100 GeV for proton/neutron spectra.

The FFD efficiencies $\epsilon(E)$, together with calculated proton or neutron energy spectra, $N(E)$, are used to generate predicted track densities. These values are then compared with measured track densities, for an evaluation of the calculated spectra and determination of LDEF fluences and doses.

EXPERIMENT

The aluminum canisters containing the A0015 detectors had acrylic liners with inner dimensions of 9.7 cm diameter by 8.6 cm depth. The detectors were 7 cm × 7 cm in dimension (with corners clipped)

151

Table 1: Shielding of LDEF A0015 Fission Foil Detectors.

Canister	Plate	Min. Vertical Shielding (g/cm^2) Al Equivalent	Min.-Max. Horizontal Shielding (g/cm^2) Al Equivalent
#1	^{209}Bi	12.7	2.75 - 10.0
	^{181}Ta	13.1	2.70 - 22.6
	^{232}Th	13.4	1.87 - 8.92
	^{238}U	13.6	1.87 - 13.4
#2	^{209}Bi	1.65	2.75 - 10.0
	^{181}Ta	1.42	2.70 - 22.6
	^{232}Th	1.20	1.87 - 8.92
	^{238}U	0.97	1.87 - 13.4

Canister #1 was located on the Earthside end of LDEF and Canister #2 near the trailing edge (Tray C2).

and were stacked through the depth of the canisters. The FFDs were contained in cutouts in acrylic plates. The shielding of the FFDs is given in Table 1. The aluminum equivalent values are given but most of the volume of the canisters was filled with plastics (polycarbonate, acrylic and CR-39). This has a significant effect on the scattering of neutrons in the vicinities of the FFDs. FFDs are at one end of the detector arrays and, from the shielding in Table 1, it is seen that the FFDs were oriented toward space in Canister #2 (trailing edge) but away from space in Canister #1 (Earthside). There were 6-10 cm^2 of each of the four foil types in each canister.

After the return of LDEF, the FFDs were removed from the canisters and disassembled. The mica films were processed in 50% HF solution at 21°C for 1.25 hr in order to delineate the fission fragment tracks for counting. The mica was given a pre-flight processing for 3 hr to enlarge the fossil tracks. The films were then counted under an optical microscope at 200×.

MEASUREMENTS

The average track densities from the mica films are given in Table 2. The standard deviations given are due to counting statistics. In addition, there were differences of up to 16% from the mean in track densities across the detector layers in Canister #1 and up to 37% in Canister #2 which seem to have been due mainly to shielding differences through the sides of the canisters. The larger gradients in track densities in Canister #2 would be expected near the trailing edge of LDEF and under smaller shielding.

It is of interest to note that the track density ratios between Canisters #1 and #2 change very little for the four foil types. Since the foils have different threshold energies one can conclude that the ratios of high energy to low energy nucleons are equal to within a few percent for the two FFD positions.

Table 2: Average Track Densities from the LDEF A0015 Fission Foil Detectors.

	Measured Track Density (cm^2)	Calculated Track Density (cm^2)
Canister #1		
^{181}Ta	131 ± 4	51.8
^{209}Bi	2340 ± 47	103
^{232}Th	23880 ± 240	9870
^{238}U	34490 ± 500*	18800
Canister #2		
^{181}Ta	148 ± 5	49.0
^{209}Bi	2825 ± 5	2030
^{232}Th	27030 ± 315	20300
^{238}U	39490 ± 500	34600

*Corrected for spontaneous fission background and surface oxidation of foils.
Canister #1 – Earthside
Canister #2 – Trailing Edge
The calculated track densities are based on proton and neutron spectra derived from primary/secondary particle propagation in a simple slab (one-dimensional) shield.

CALCULATIONS

Numerical integrations were carried out, as discussed above, to calculate theoretical track densities for comparison with measurements. These results are approximate since the simple slab geometry models developed by Armstrong and Colborn[1] were used to propagate the incident particles through shielding. Secondary particles are included in the calculations.

The equation for numerical integration is

$$D_c = \sum_{E_{min}}^{E_{max}} \epsilon_p(E)N_p(E) + \sum_{E_{min}}^{E_{max}} \epsilon_n(E)N_n(E) \tag{1}$$

where ϵ_p and ϵ_n are the detector efficiencies for protons and neutrons, respectively (Figure 2), and N_p and N_n are the calculated proton and neutron spectra in the vicinity of the FFDs. An example of the proton and neutron spectra for a slab thickness of 10 g/cm^2 Al is given in Figure 3.

The calculated track densities for each of the four FFD types as functions of slab thickness are plotted in Figure 4 with the measurements. Values corresponding to the vertical shielding of the FFDs in Table 1 are given in Table 3 along with the measurements. There is better agreement between calculation and measurement for Canister #2, where the shielding is small. For thicker shielding the slab calculations fall well under the canister measurements because of the large difference in shielding from the sides.
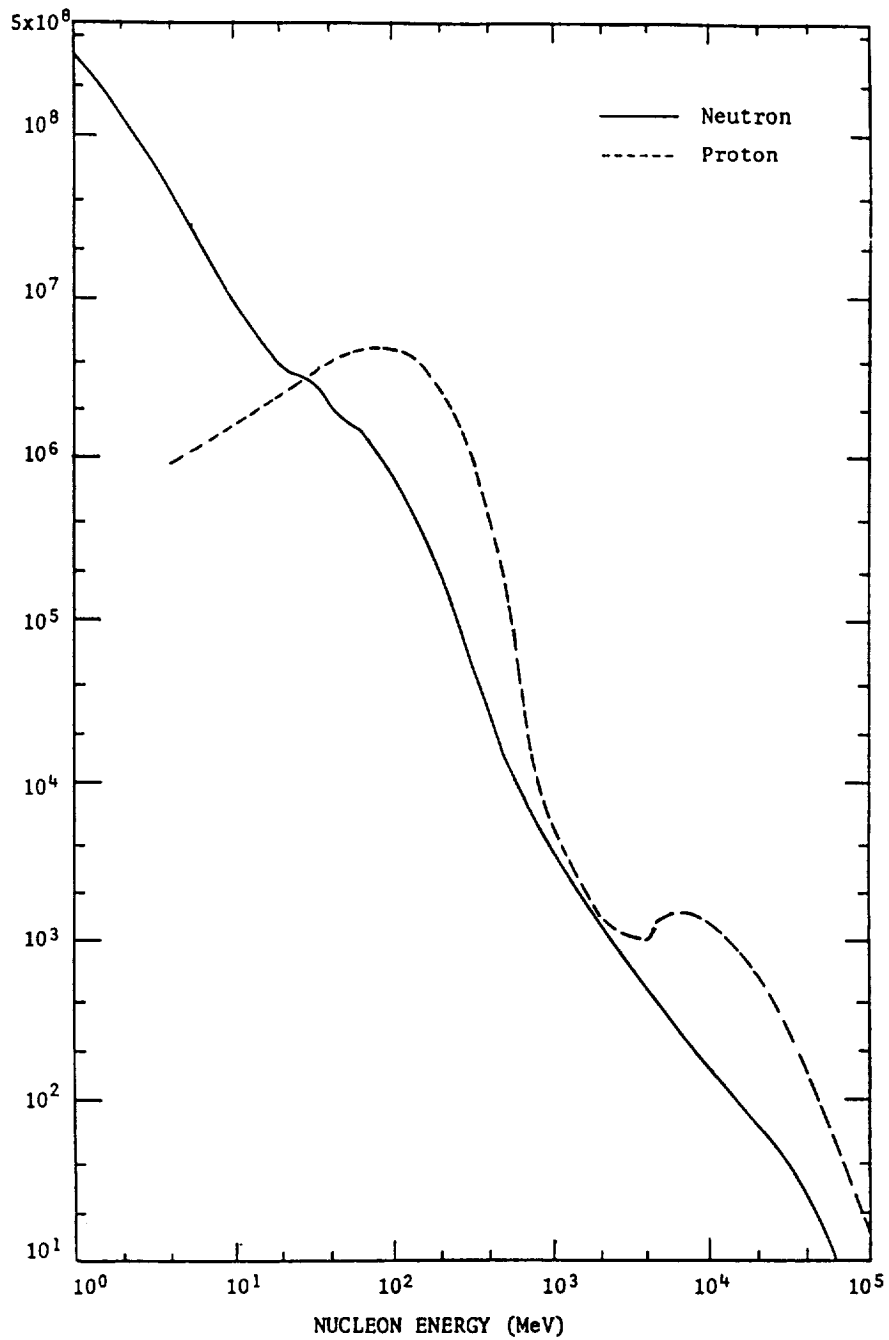
Figure 3: Differential spectra of neutrons and protons accumulated during the total LDEF mission under 10 g/cm² Al. from data by Armstrong and Colborn (1990). Summations and extrapolations by the authors.
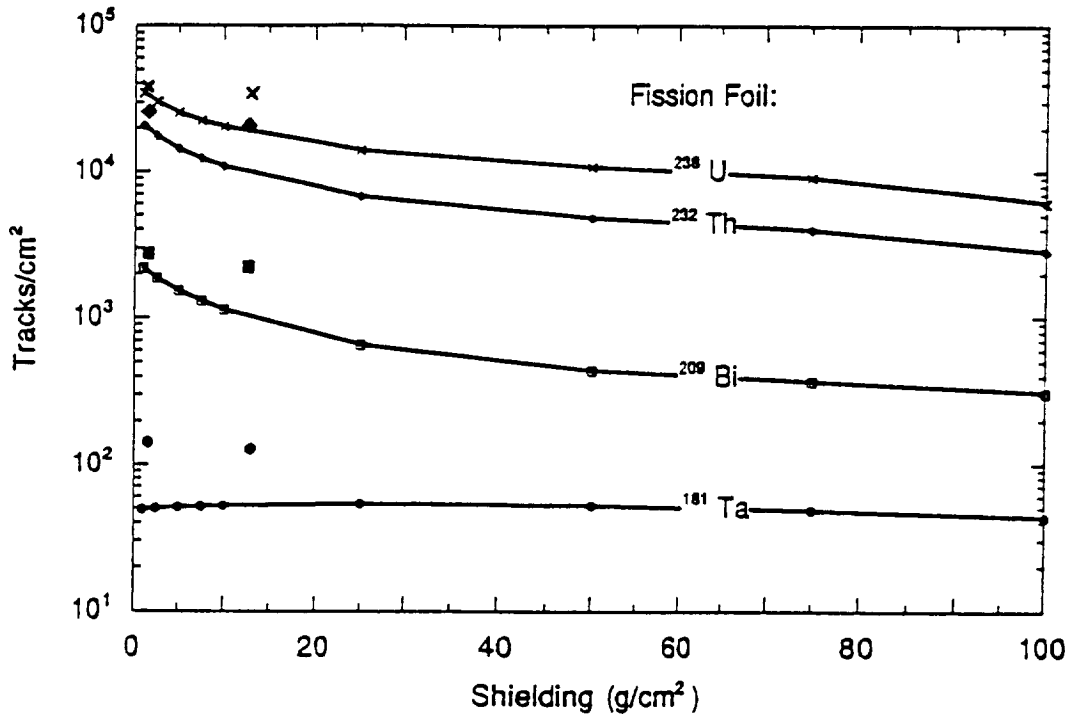
Figure 4: Calculated and measured fission fragment track densities from the combined p,f and n,f reactions in the A0015 fission foil detectors on LDEF. The calculations are based on a simple 1-D (slab) geometry (Armstrong and Colborn, 1990). The measured values lie at approximately 1 and 13 g/cm^2.

The calculations for Canister #2 are low by 67, 28, 25 and 12% for ^{181}Ta, ^{209}Bi, ^{232}Th and ^{238}U, respectively. The higher the energy threshold, the greater the deviation. This suggests that the calculated proton and neutron energy spectra may be deficient at higher energies.

The proton absorbed doses and the neutron dose equivalents have been approximated for the FFD measurements by scaling the calculated proton and neutron track densities to the total measured values. The proton dose, in rad, is given by

$$D = 1.602 \times 10^{-8} \sum_{E_1}^{E_2} N(E) \frac{dE}{dx} \tag{2}$$

where E_1 and E_2 are 10 MeV and 100 GeV, the energy end points in this study. $N(E)$ is the differential proton spectrum in cm^{-2} MeV^{-1} and $\frac{dE}{dx}$ is the energy absorption of protons in tissue in MeV cm^2 g^{-1}.

The dose equivalent for neutrons, in rem, is given by

$$DE = 10^{-3} \sum_{E_1}^{E_2} d(E) n(E) \tag{3}$$

where E_1 and E_2 are 1 MeV and 60 GeV, $d(E)$ is the dose equivalent conversion factor in rem cm^2 and $n(E)$ is the differential neutron spectrum in cm^2 MeV^{-1}. The d values were taken from NCRP (1971) up to 500 MeV and extended to 60 GeV from that energy.

Table 3: High Energy Proton and Neutron Doses for the A0015 Fission Foil Detectors.

Canister	Position	Shielding (g/cm²) Al Equivalent	Proton Dose (rad)	Neutron Dose (rem)	TLD Proton Dose (rad)
1	Earthside	13.2	171	82	200
2	Trailing Edge	1.3	315	33	500

The doses were determined by scaling calculated values of proton and neutron induced track densities to total measured values.

The doses correspond to proton energies of 10 MeV to 100 GeV and neutron energies of 1 MeV to 60 GeV.

The doses are given in Table 3. The proton doses can be compared to measured TLD doses in the same canisters. Extrapolating from the shielding dose distribution measured with TLDs, we would expect about 225 rad in Canister #1 and 550 rad in Canister #2. About 90% of these doses would be due to protons in the energy range of the FFDs. The TLD proton doses are therefore about a factor of 1.2 higher in Canister #1 and 1.6 higher in Canister #2. Given the approximations involved in the slab calculations of proton and neutron spectra and simple scaling of track densities to get measured proton doses, these differences are within expectations.

DISCUSSION

A comparison has been made between fission foil detector measurements (track densities) induced by proton/neutron fluences encountered on LDEF and predicted track densities based on calculated proton and neutron spectra. The calculations employed a simple slab geometry[1]. The predicted track densities on the detectors were less than measurements by ~25% at 1 g/cm² shielding (trailing edge) and more than a factor of 2 at 13 g/cm² (Earthside). The differences are primarily due to the slab geometry approximation of actual spaceflight conditions. Future calculations based on a geometrical model of the A0015 experiment are needed for a more accurate test for the radiation modeling code.

The proton doses derived by combining measurements and calculations were 16% and 37% less than TLD doses measured in the flight canisters, when extrapolated to equivalent shielding. The differences can be explained by the approximations involved in the calculations.

In Table 4 the A0015 neutron dose equivalent rates are compared with measurements from other spaceflights. The LDEF rates are seen to be higher than all other measurements, by factors of approximately 6 to 40. The primary reason for the large differences is in the greater LDEF flight altitude, with higher primary proton and secondary neutron fluxes. Shielding differences may also play a significant role.

156

Table 4: Spaceflight High Energy (>1 MeV) Neutron Measured Comparisons.

Space flight	Experi- ment	Shielding	Altitude (km)	Incli- nation	Dose Equiv. Rate (mrem/d)
LDEF	A0015	1 g/cm²	478	28.5°	16
	A0015	13 g/cm²			39
	P0006	17 g/cm²			33
STS-9(SL-1)	VFI	Pallet	241	57°	4.2
STS-51F(SL-2)	VFI	Pallet	322/304	49.5°	4.0
STS-3		Locker	280	40.3°	0.95
STS-4		Locker	297	28.5°	1.3
STS-5		Locker	284	28.5°	2.2
STS-6		Locker	293	25.5°	1.3
Cosmos 936	Inside Spacecraft		419/224	62.8°	6.8
Cosmos 1129	Inside Spacecraft		394/226	62.8°	6.8
Cosmos 2044	Outside Spacecraft		294/216	82.3°	3.3

Due to approximations made in separating neutron and proton contributions to the fission foil detector measurements, the accuracy of neutron dose equivalents is estimated to be within a factor of 3.

REFERENCES

1. Armstrong T.W. and B.L. Colborn, *Scoping estimates of the LDEF satellite induced radioactivity*, SAIC, Report No. SAIC-90/1462, 1990.

2. Benton E.V., R.M. Cassou, A.L. Frank, R.P. Henke and D.D. Peterson, "Space radiation on board Cosmos 936–U.S. portion of experiment K206," *Final Reports of U.S. Plant and Radiation Experiments Flown on the Soviet Satellite Cosmos 936*, (S.N. Rosenzweig and K.A. Souza, eds.). NASA TM 78526, 1978.

3. Benton E.V., R.P. Henke, A.L. Frank, C.S. Johnson, R.M. Cassou, M.T. Tran and E. Etter, "Space radiation dosimetry aboard Cosmos 1129–U.S. portion of experiment K309," *Final Reports of U.S. Plant and Radiation Experiments Flown on the Soviet Satellite Cosmos 1129* (M.R. Heinrich and K.A. Souza, eds.) NASA TM 81288, 1981.

4. Benton E.V., R.P. Henke, A.L. Frank, R.M. Cassou, C.S. Johnson and M.T. Tran, *Final Dosimetry Reports for STS-3, STS-4, STS-5, STS-6, TR-54, -56, -57, -58*, University of San Francisco Physics Research Laboratory, 1982-1983.

5. Dudkin V.E., Yu.V. Potapov, A.B. Akopova, L.V. Melkumyan, Sh.B. Rshtuni, E.V. Benton and A.L. Frank, "Neutron fluences and energy spectra in the Cosmos-2044 Biosatellite orbit," *Nucl. Tracks Radiat. Meas.*, Vol. 20, No. 1, pp. 139-141, 1992.

6. Frank A.L., E.V. Benton, E.R. Benton, V.E. Dudkin and A.M. Marenny, *Radiation experiments on Cosmos 2044: K-7-41, Parts A,B,C,D,E,* TR-76, University of San Francisco Physics Research Lab, 1990.

7. Lomanov M.F., G.G. Shimchuk and R.M. Yakovlev, "Solid state detectors of fission fragments for the REM dose measurement of mixed proton and neutron radiation," *Hlth. Phys.* Vol. 37, pp.677-686, 1979.

8. Pretre S., E. Tochilin and N. Goldstein, "A standardized method for making neutron fluence measurements by fission fragment tracks in plastics," *Proc. 1st International Congress on Radiation Protection,* Rome, 1968.

9. Stehn J.R., M.D. Goldberg, R. Wiener-Chasmon, S.F. Mughabghab, B.A. Magurno and V.M. May, *Neutron Cross Sections* Vol.III, BNL 325, 1965.

10. Wollenberg H.A. and A.R. Smith, *Energy and flux determinations of high energy nucleons,* UCRL 19364, 1969.